Supplementary Information for
Geothermal heating affecting ocean stratification and circulation after the Last Glacial Maximum

Ming Zhang[1], Qi Cui[2], Yonggang Liu[2,3*], Jiang Zhu[4], Zhuoqun Wang[2], Gerrit Lohmann[5,6*]

[1]*National Supercomputing Center in Shenzhen, Shenzhen, China*

[2]*Laboratory for Climate and Ocean-Atmosphere Studies, Department of Atmospheric and Oceanic Sciences, School of Physics, Peking University, Beijing, 100871, China*

[3]*Institute of Ocean Research, Peking University, Beijing, 100871, China*

[4]*Climate and Global Dynamics Laboratory, National Center for Atmospheric Research, Boulder, CO, USA*

[5]*Alfred Wegener Institute, Helmholtz Centre for Polar and Marine Research, Bremerhaven, Germany*

[6]*University of Bremen, Bremen, Germany*

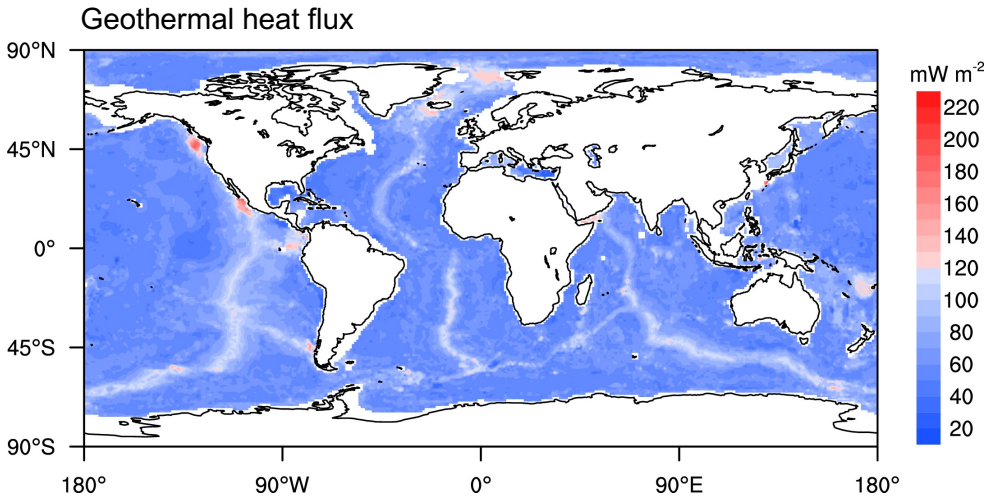

Figure. S1. Distribution of the geothermal heat fluxes at the sea floor (units: mW m^{-2}) from Goutorbe et al. (2011).

Table. S1. Summary of the experiment parameters and results.

Experiment	LGMCtl	LGMGHFd	LGMGHFg	LGMGHFd_in
Orbit	21 ka	21 ka	21 ka	21 ka
CO_2 (ppm)	185	185	185	185
CH_4 (ppb)	350	350	350	350
N_2O (ppb)	200	200	200	200
Ice sheets	ICE-6G	ICE-6G	ICE-6G	ICE-6G
Topography coastlines	ICE-6G	ICE-6G	ICE-6G	ICE-6G
Geothermal heating	none	Davies 2013	Goutorbe et al., 2011	Davies 2013
Duration (year)	4000	4000	2200	1000
GMST (°C)	7.66	8.15	7.89	-
AMOC strength (Sv)*	24.79	24.19	24.72	-
AMOC depth (m)*	2866	2991	2919	
AABW strength (Sv)*	-9.48	-10.32	-9.85	-
GMST trend (°C/kyr)*	0.06	0.11	0.13	-
AMOC trend (Sv/kyr)*	-0.18	-0.26	-0.33	-
Atlantic stratification (N^2, 10^{-6} s^{-2})*	6.09	5.90	6.00	-
Pacific stratification (N^2, 10^{-6} s^{-2})*	9.50	9.42	9.41	-
Global ocean stratification (N^2, 10^{-6} s^{-2})*	7.12	7.00	7.03	-

* The AMOC strength is defined as the maximum Atlantic meridional streamfunction (AMSF) below 500 m depth. The AMOC depth is diagnosed as the depth of zero streamfunction between 1000 and 3500 m in the Atlantic. The AABW strength is defined as the minimum globally meridional streamfunction (GMSF) below 3000 m depth. The GMST and AMOC trend are calculated based on the last 1000 years of simulations. The stratification is represented by the Brunt-Vaisala frequency (N^2, $N^2(z) = -\frac{g}{\rho_0}\frac{d\rho(z)}{dz}$). N^2>0, as density increases with depth.

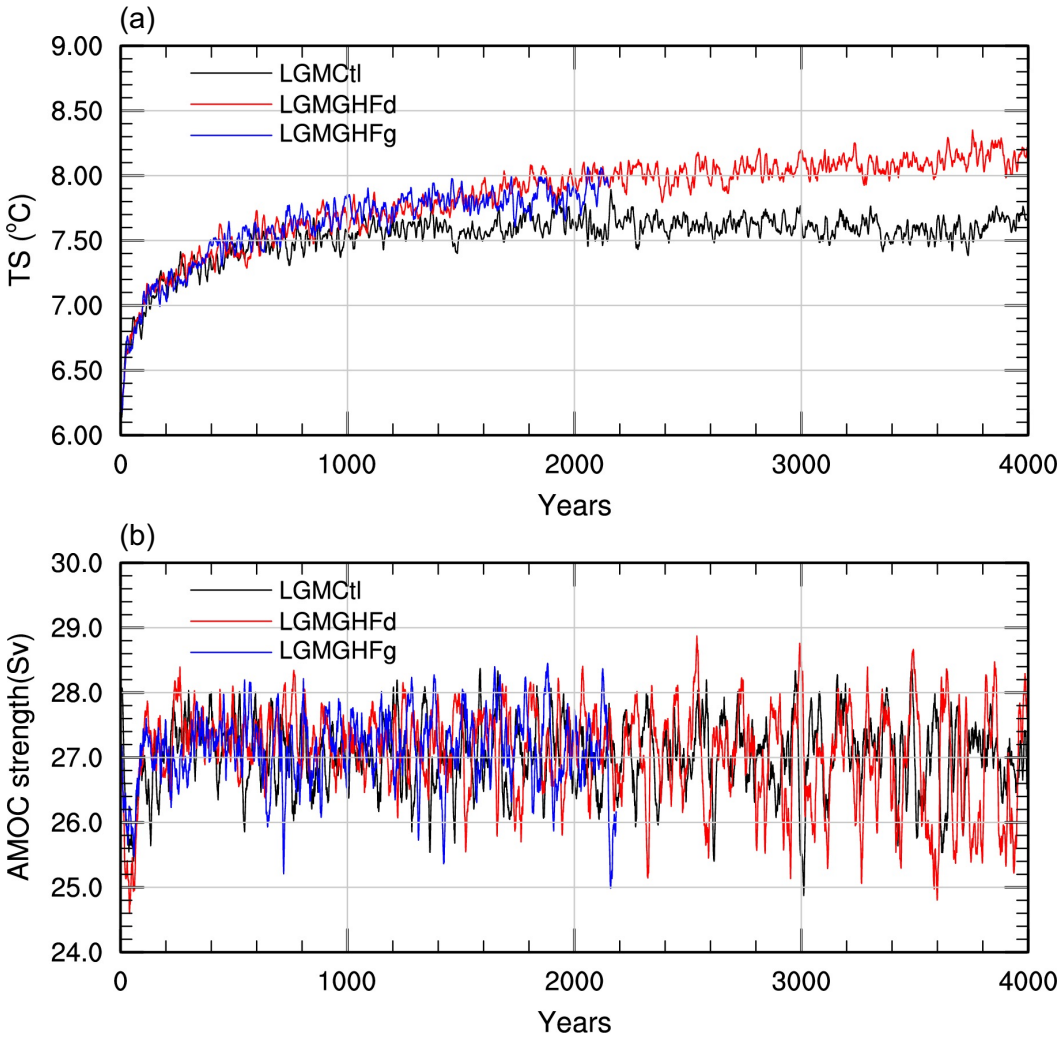

Figure. S2. Evolution of (a) globally annual mean surface temperature (unit: ℃) and (b) AMOC strength (defined as the maximum Atlantic meridional streamfunction below 500 m depth, unit: Sv) in the experiments of LGMCtl, LGMGHFd and LGMGHFg. A 10-yr running mean filter has been applied to all curves.

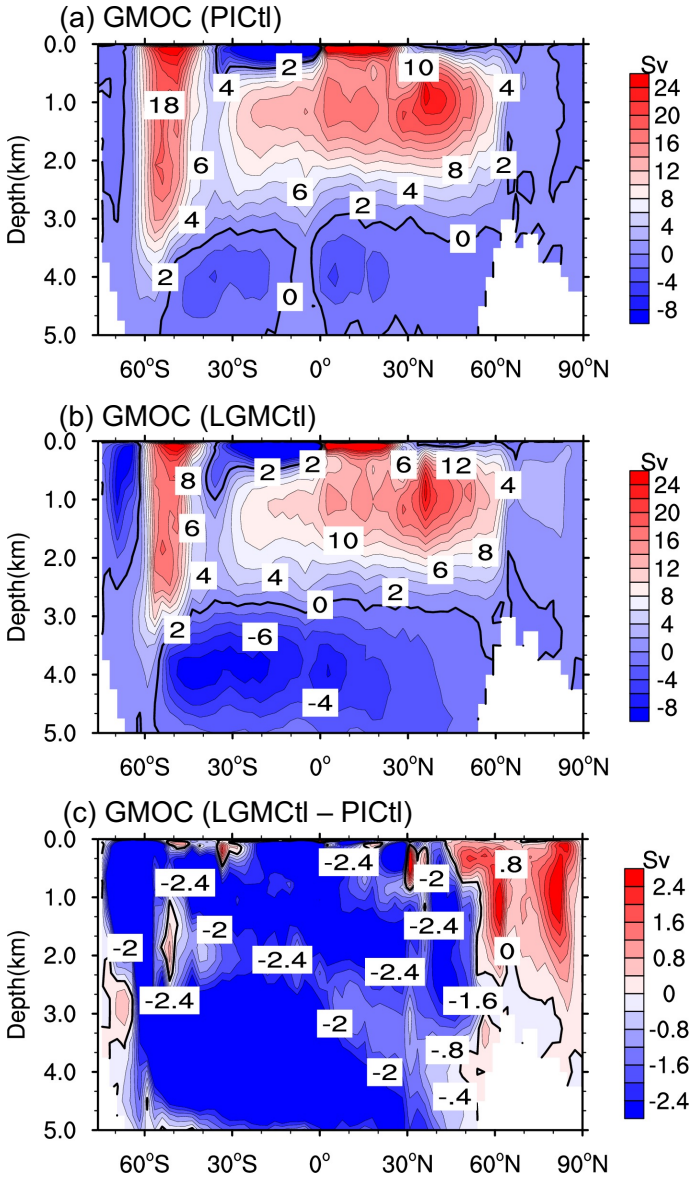

Figure S3. Global meridional ocean circulation (GMOC, units: Sv) for PI and LGM is shown in (a) and (b), respectively. GMOC difference between LGM and PI is shown in (c). Zero contour lines are indicated in black.

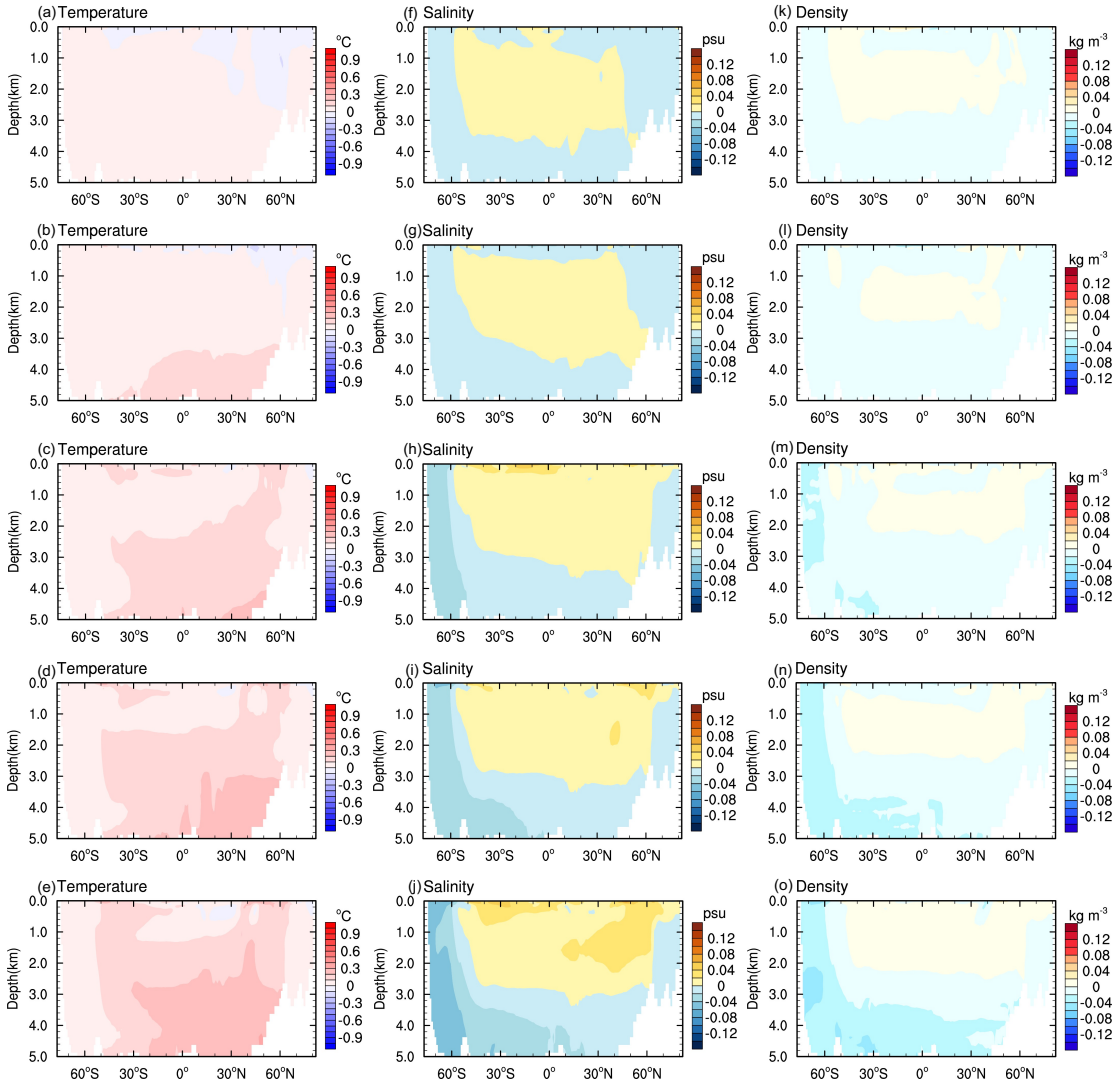

Figure S4. Changes of zonal-mean (a-e) potential temperature (units: ℃), (f-j) salinity (units: psu) and (k-o) potential density (units: kg m^{-3}) in the Atlantic Ocean averaged over (a, f, k) year 1-200; (b, g, l) year 201-400; (c, h, m) year 401-600; (d, i, n) year 601-800; (e, j, o) year 801-1000 after adding the geothermal heat flux. Part of the Southern Ocean over 70°W-20°E is included.

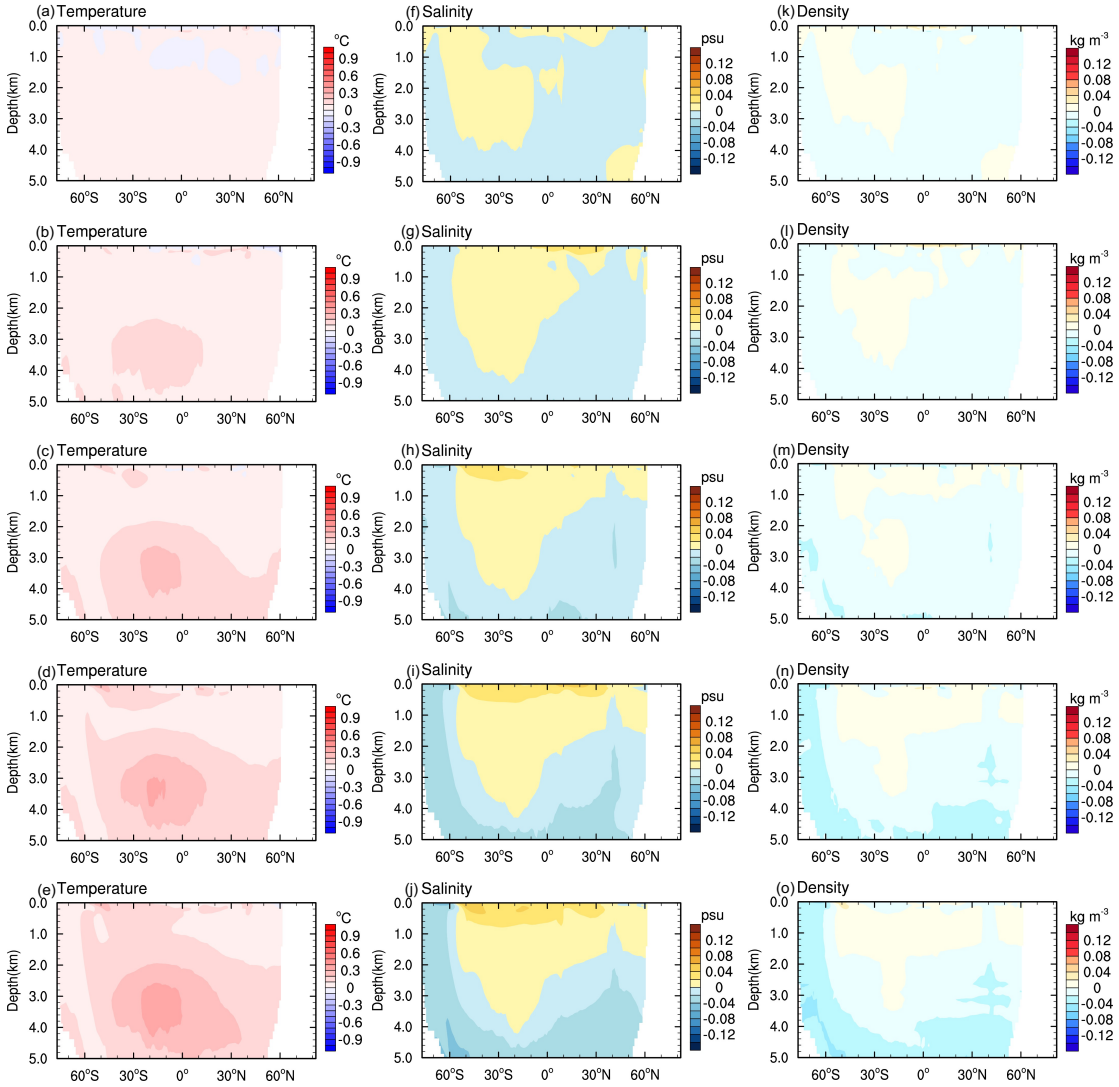

Figure. S5. Changes of zonal-mean (a-e) potential temperature (units: ℃), (f-j) salinity (units: psu) and (k-o) potential density (units: kg m^{-3}) in the Pacific Ocean averaged over (a, f, k) year 1-200; (b, g, f) year 201-400; (c, h, m) year 401-600; (d, i, n) year 601-800; (e, j, o) year 801-1000 after adding the geothermal heating. Part of the Southern Ocean over 130°E-180° and 180°-70 °W is included.

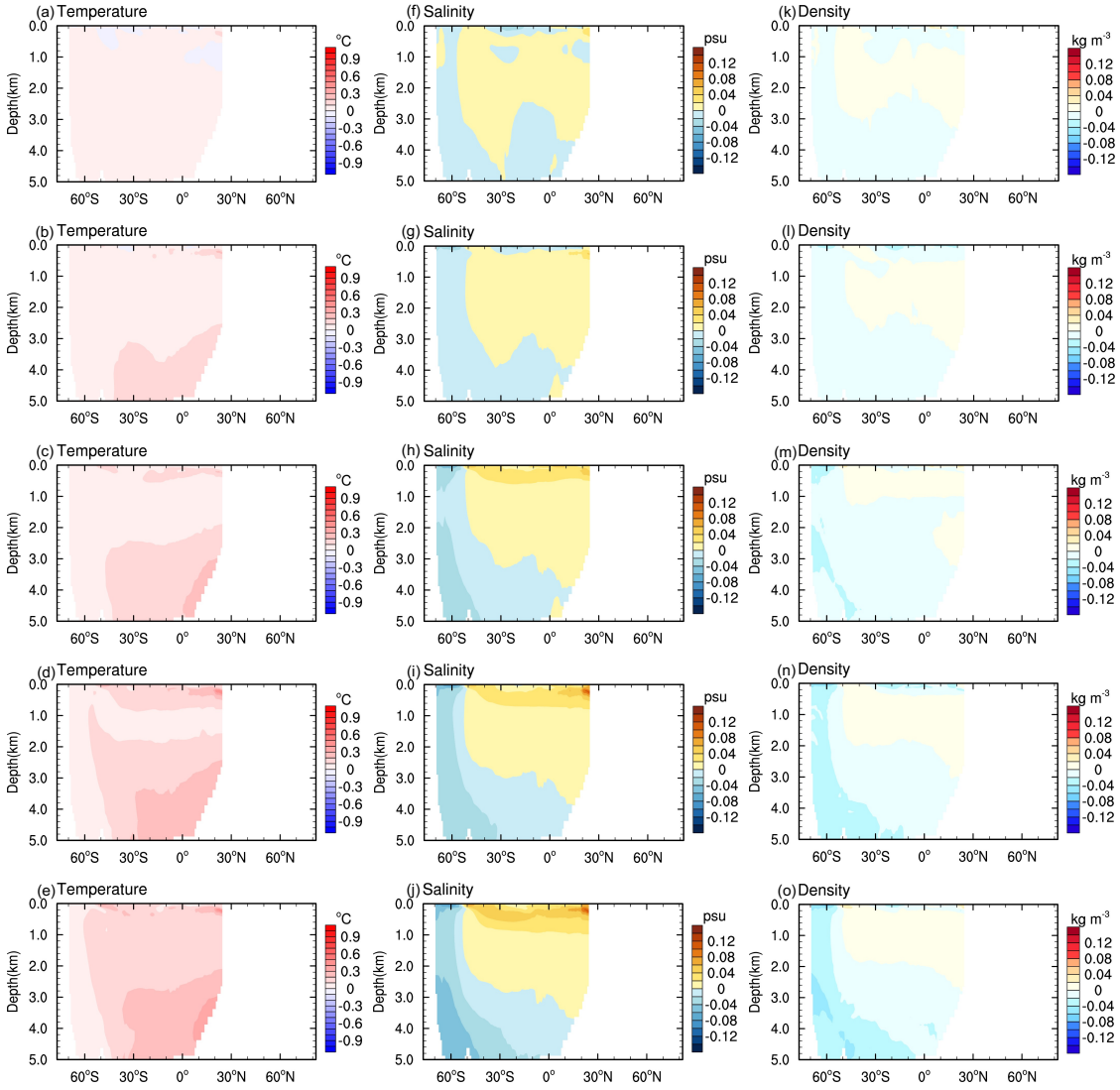

Figure. S6. Changes of zonal-mean (a-e) potential temperature (units: ℃), (f-j) salinity (units: psu) and (k-o) potential density (units: kg m^{-3}) in the Indian Ocean averaged over (a, f, k) year 1-200; (b, g, f) year 201-400; (c, h, m) year 401-600; (d, i, n) year 601-800; (e, j, o) year 801-1000 after adding the geothermal heating. Part of the Southern Ocean between 20 ºE and 130 ºE is included.

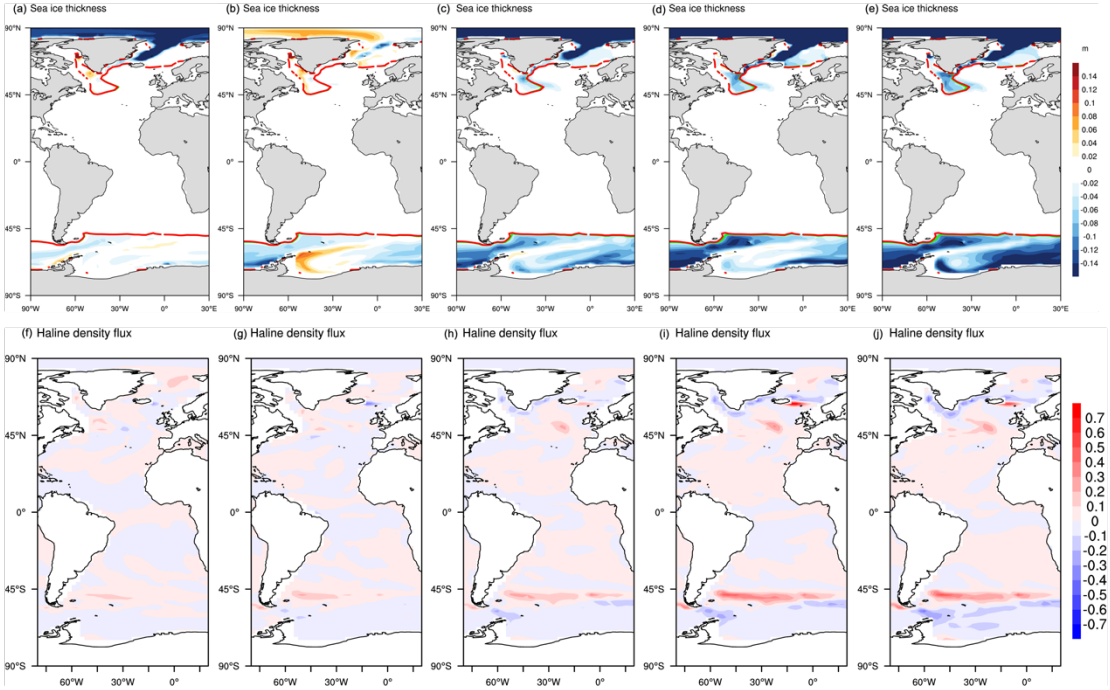

Figure. S7. Changes in annual mean (a-e) sea ice thickness (in color, units: m) and (f-j) haline density flux (units: 10^{-6} kg m^{-2} s^{-1}) averaged over (a, f) year 1-200; (b, g) year 201-400; (c, h) year 401-600; (d, i) year 601-800; (e, j) year 801-1000 after adding the geothermal heat flux. The sea-ice margin (defined as the 15 % sea ice-fraction) in the Atlantic Ocean in both LGMCtl and LGMGHFd are shown in red and green contours (a-e), respectively.

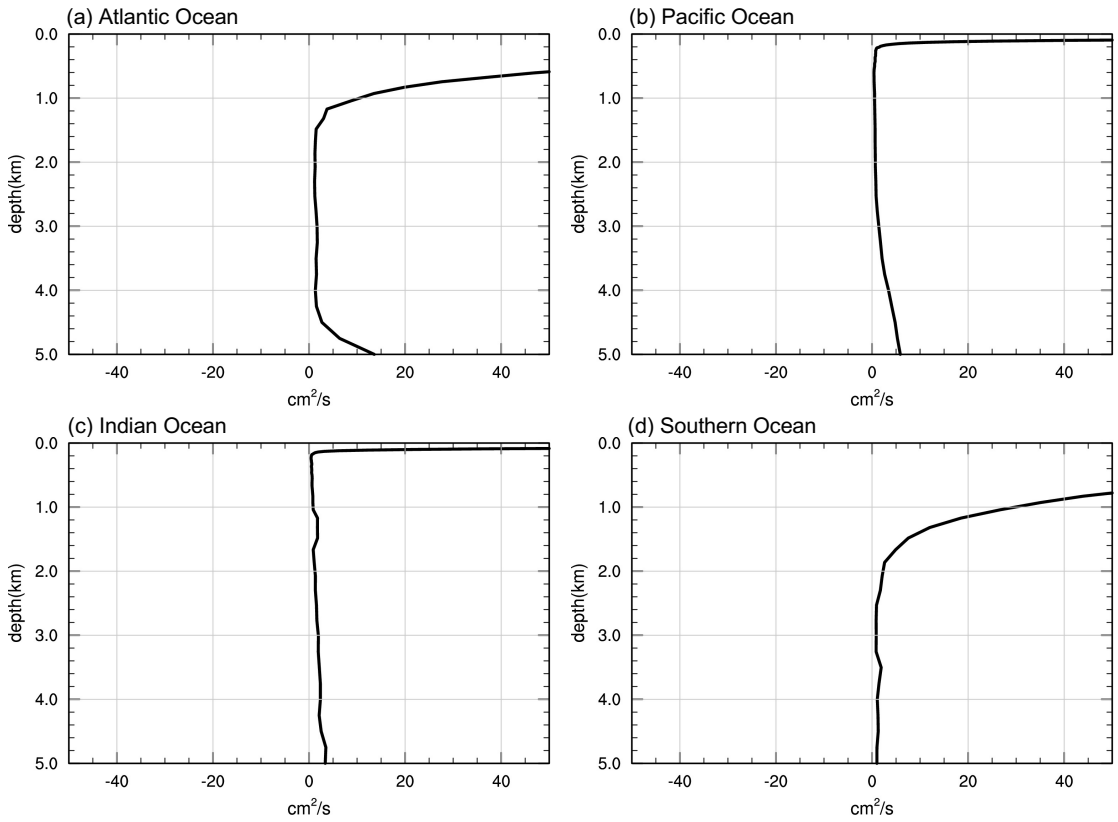

Figure. S8. Annual-mean vertical diffusivity coefficient (units: cm^2/s) in the (a) Atlantic Ocean, (b) Pacific Ocean, (c) Indian Ocean and (d) Southern Ocean in the control experiment (LGMCtl).

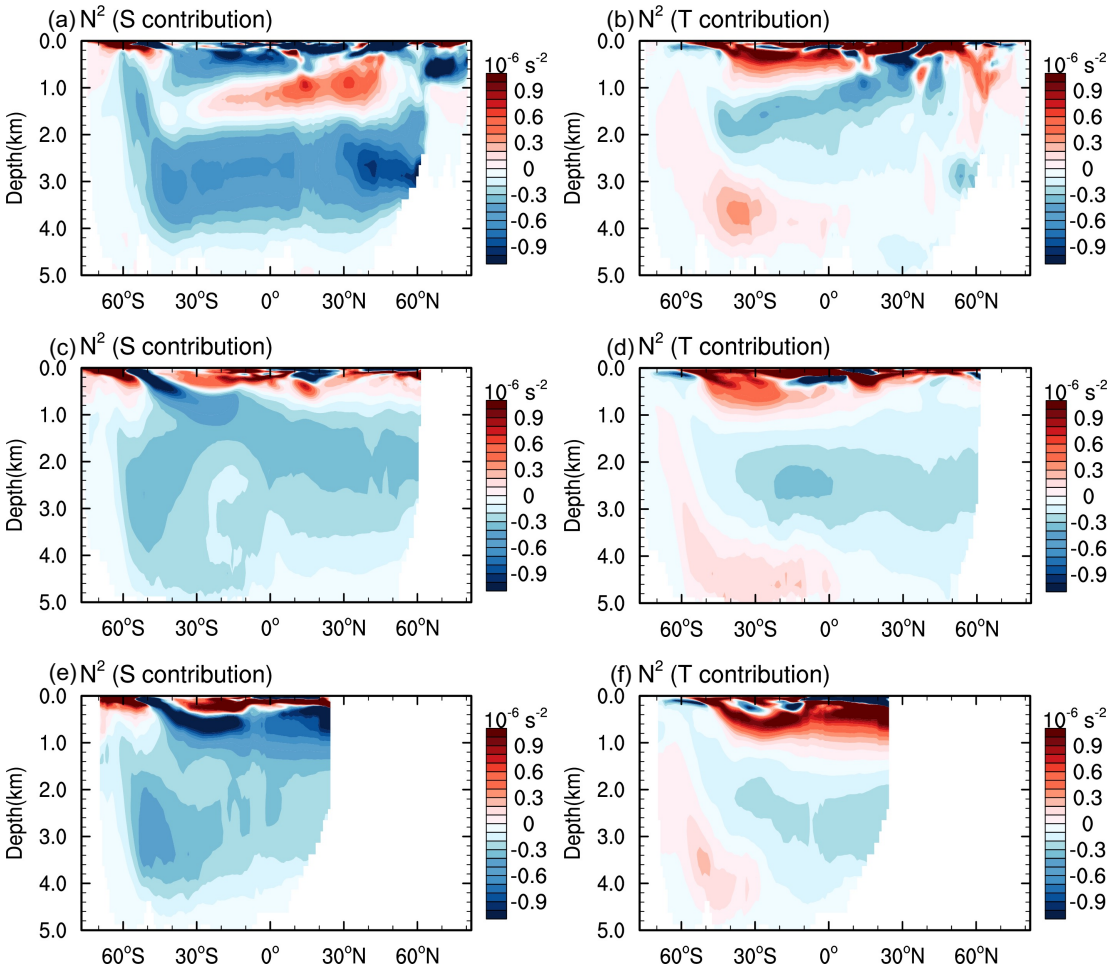

136

137 **Figure. S9.** Changes in zonal mean Brunt-Vaisala frequency (N^2, units: 10^{-6} s^{-2})

138 contributed by salinity (a, c, e) and temperature (b, d, f) in the Atlantic Ocean (a-b),

139 Pacific Ocean (c-d) and Indian Ocean (e-f) for the experiment LGMGHFd compared

140 to LGMCtl. Part of the Southern Ocean within the longitude range of the Atlantic

141 Ocean, Pacific Ocean and Indian Ocean is included.

142

143

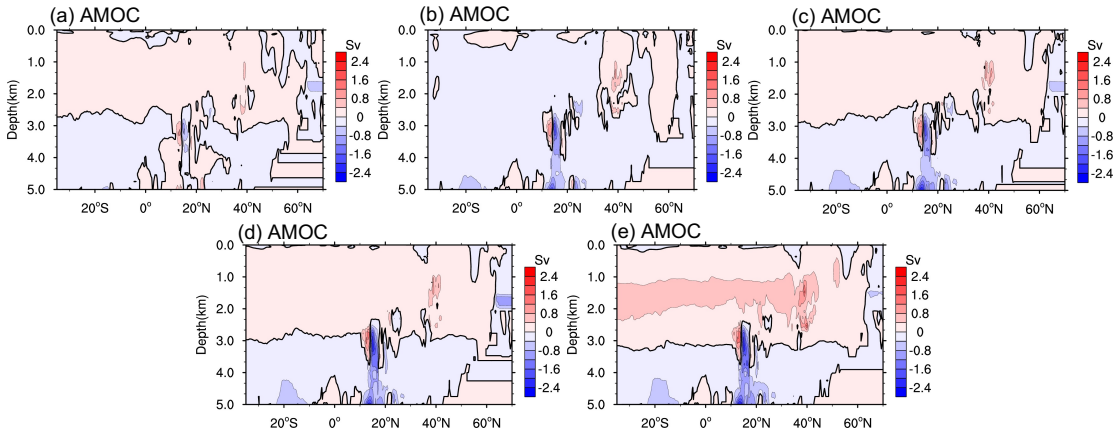

144

145 **Figure. S10.** Change in annual mean AMSF (units：Sv) averaged over (a) year 1-

146 200, (b) year 201-400, (c) year 401-600, (d) year 601-800 and (e) year 801-1000 after

147 adding the geothermal heat flux. Zero contour lines are indicated in black.

148

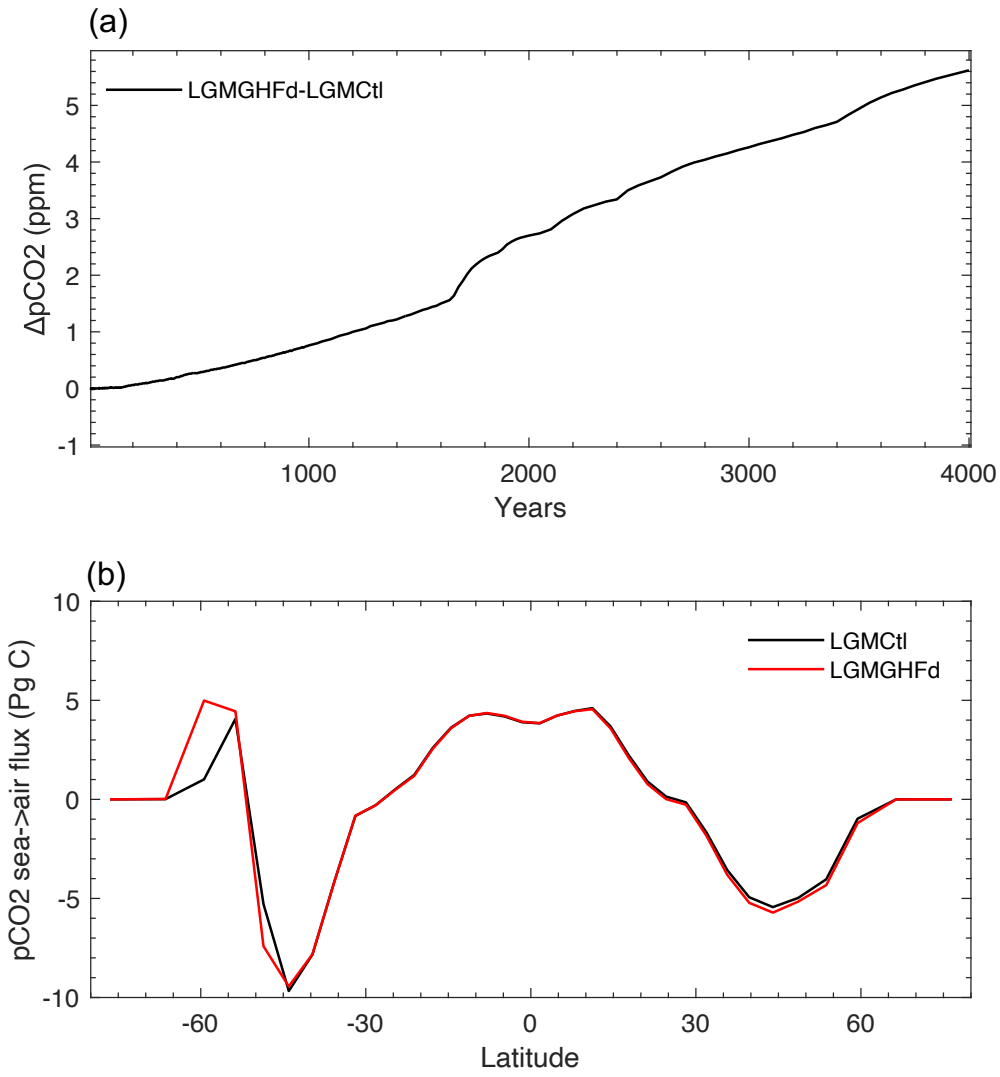

Figure. S11. Influence of geothermal heating on pCO_2 during the LGM simulated using cGENIE. (a) evolution of pCO_2 after the geothermal heating (Fig. 2a) is turned on. (b) the zonally integrated sea-to-air fluxes of CO_2 when the geothermal heating is off (black curve) and on (red curve).